IEEE Access
Multidisciplinary | Rapid Review | Open Access Journal

Received September 16, 2019, accepted October 6, 2019, date of publication October 23, 2019, date of current version November 5, 2019.

Digital Object Identifier 10.1109/ACCESS.2019.2949217

Parallel Quadrature Spatial Modulation for Massive MIMO Systems With ICI Avoidance

GUOSHENG HUANG[1,2], CHUANPING LI[2], SONIA AÏSSA[3], (Fellow, IEEE), AND MINGHUA XIA[2], (Member, IEEE)

[1]School of Information Science and Engineering, Hunan First Normal University, Changsha 410205, China
[2]School of Electronics and Information Technology, Sun Yat-sen University, Guangzhou 510006, China
[3]Institut National de la Recherche Scientifique (INRS), University of Quebec, Montreal, QC H5A 1K6, Canada

Corresponding author: Guosheng Huang (hgsheng@mail.sysu.edu.cn)

This work was supported in part by the Major Science and Technology Special Project of Guangdong Province under Grant 2018B010114001, in part by the Natural Science Foundation of Hunan Province under Grant 11JJ6061, and in part by the Science Research Foundation of Hunan Provincial Department of Education under Grant 20192911058.

ABSTRACT Despite its efficiency in conventional multiple-input multiple-output (MIMO) wireless systems, quadrature spatial modulation (QSM) becomes less efficient in massive MIMO systems since it does not adapt to the number of antennas but always uses one or two out of them. To adopt QSM in massive MIMO systems, a parallel quadrature spatial modulation (PQSM) scheme is proposed in this paper. In PQSM, the transmit (Tx) antennas are divided equally into $P > 1$ groups, and the bit sequence to be transmitted during a time slot is divided into $P + 1$ parts. Then, the first part is applied to map an M-QAM complex constellation symbol while the remaining P parts of the bitstream are used to perform P QSMs in parallel. By allowing a tradeoff between the spatial modulation order and signal constellation order, PQSM enables lower bit error rate (BER) with no loss of spectral efficiency compared with QSM. For a fixed signal constellation, PQSM yields higher spectral efficiency than QSM since more selected antenna indices can carry more data bits. The algorithm pertaining to the proposed scheme is designed, and an upper bound on the average bit error rate (ABER) is derived. Moreover, to minimize the ABER, an algorithm is developed to optimize the number of Tx antenna groups and the signal constellation order. Monte-Carlo simulation results demonstrate the superiority of PQSM over generalized SM and QSM, as well as the effectiveness of the developed performance analysis.

INDEX TERMS Average bit error rate, inter-channel interference, massive multiple-input multiple-output, parallel quadrature spatial modulation, spectral efficiency.

I. INTRODUCTION

Since massive multiple-input multiple-out (MIMO) technology can greatly improve system capacity and spectral efficiency, it is widely recognized as a key technology in 5G and beyond wireless communication systems [1]. The traditional MIMO technologies, such as Vertical Bell Labs layered space-time (V-BLAST) schemes, break input data stream into multiple sub-streams that are transmitted through multiple antennas, and consequently the spectral efficiency increases linearly with the number of transmit (Tx) antennas. However, V-BLAST-based MIMO systems suffer from high inter-channel interference (ICI) at the receiver. The detection algorithm for reducing ICI in massive MIMO systems is very complicated, and the high ICI would degrade system performance [2]. Therefore, how to effectively improve spectral efficiency through multiple antennas and avoid ICI becomes a challenging problem in massive MIMO. The spatial modulation (SM) based MIMO techniques provide an inspiring solution [3]. In principle, SM introduces an extra spatial dimension into MIMO systems, and extends digital modulation from two-dimensional mapping to three-dimensional mapping. That is, data bits are transmitted not only by the mapped signal constellation symbols (i.e., data symbols), but also by the selected antenna indices (i.e., spatial symbols) [4].

During a transmission time slot, the original SM scheme [3] selects one antenna out of all Tx antennas and transmits data symbol through a single radio frequency (RF) link. Although it is able to avoid ICI and inter-symbol

The associate editor coordinating the review of this manuscript and approving it for publication was Min Li.

interference (ISI), its spectral efficiency can only increase logarithmically rather than linearly with the number of Tx antennas. To exploit more Tx antennas, generalized spatial modulation (GSM) was studied in [5], [6], where a combination of multiple Tx antennas is used as a spatial symbol. Since GSM uses multiple active antenna indices to encode information bits, it enables higher spectral efficiency than SM. Moreover, in GSM, the same data symbols are transmitted through different antennas, so it can effectively avoid ICI and ISI.

Quadrature spatial modulation (QSM) proposed in [7] is a new method to enhance the overall spectral efficiency of the SM technique while retaining almost all inherent advantages of SM systems. In QSM, each complex data symbol is divided into real and imaginary parts, which are simultaneously transmitted to the receiver by two mutually orthogonal carriers over one or two antennas depending upon the subsequent data bits [8]. For a MIMO system with N_t Tx antennas and M-QAM constellation adopted, QSM provides $\log_2(N_t)$ bits per channel use (bpcu) improvement in spectral efficiency compared with the original SM whose spectral efficiency is $\log_2(N_t M)$ bpcu [3]. Moreover, since two mutually orthogonal carriers are used in QSM, ICI is completely avoided [9]. As a result, QSM is widely recognized as a promising technique for future wireless communications systems and has attracted significant research interest in recent years. To name just a few, the performance of QSM over Nakagami-m fading channels was studied in [10], whereas a comprehensive framework for QSM in generalized fading scenarios was investigated in [11]. The impact of co-channel interference on QSM was explored in [12] and a differential QSM was introduced in [13]. Also, an anti-eavesdropping scheme was designed for QSM in [14] and the performance of QSM in cognitive radio systems was studied in [15]. To further improve the performance of QSM, the minimum Euclidean distance of signal symbols was increased in [16] and the signal space diversity was exploited in [17]. Application of QSM to 5G outdoor millimeter-wave communications was reported in [18]. Very recently, a precoding aided QSM was proposed in [19], where the precoding matrix is designed to preprocess the in-phase and quadrature signals of QSM. Also, the secure transmission for differential QSM with artificial noise was investigated [20].

Despite its efficiency in conventional MIMO systems, QSM becomes less efficient in massive MIMO systems since it does not adapt to the number of antennas but always uses one or two out of them. Although GSM can be applied in massive MIMO systems, the number of possible Tx antenna combinations in GSM cannot be fully used for spatial symbols. For instance, if a combination of N_u out of N_t antennas is used as a spatial symbol, the number of possible antenna combinations is $N_c = \binom{N_t}{N_u}$, with $\binom{\cdot}{\cdot}$ being the binomial coefficient. Among them, only $2^{\lfloor \log_2 N_c \rfloor}$ combinations, with $\lfloor \cdot \rfloor$ being the floor operation, can be exploited to convey spatial symbols. As a result, the mapping from information bits to the possible antenna combinations is not one-to-one. Furthermore, as N_t and N_u increase, the antenna mapping table of GSM becomes very complicated [5].

To adapt QSM for massive MIMO systems, a parallel quadrature spatial modulation (PQSM) scheme is proposed in this paper. In PQSM, the Tx antennas are divided equally into $P > 1$ groups, and the bit sequence to be transmitted during a time slot is divided into $P + 1$ parts. The first part is applied to map an M-QAM complex constellation symbol, and the remaining P parts are used to perform P QSMs in parallel. Clearly, PQSM reduces to the conventional QSM when $P = 1$.

Compared with GSM and QSM, the proposed PQSM presents attractive features including, *i)* PQSM can achieve the best tradeoff between the order of signal constellation and the order of spatial modulation, thus reducing the average bit error rate (ABER); *ii)* PQSM can obtain higher spectral efficiency than conventional QSM by activating an optimal number of Tx antennas groups (denoted P_{opt}) instead of one or at most two antennas; and *iii)* By transmitting the same data symbol in parallel, PQSM retains the key advantage of SM, namely, the complete avoidance of ISI and ICI. Further, PQSM has spatial diversity gain and it is able to increase the reliability of the wireless channel, by providing replicas of the transmitted data symbol to the receiver.

In summary, the main contributions of this paper are as follows:

- A PQSM scheme is developed for massive MIMO system, and the algorithm to implement PQSM is explicitly formulated.
- An optimization algorithm is designed to get the optimal number of Tx antenna groups and the corresponding order of signal constellation in the sense of minimum ABER, achieving the best tradeoff between spatial domain and signal domain in a massive MIMO system.
- The spectral efficiency, an upper bound on ABER, and the receiver complexity of PQSM are analytically derived and compared with those of GSM and QSM. Both theoretical analysis and simulation results demonstrate the superiority of PQSM over QSM and GSM, in terms of spectral efficiency and/or ABER.

To detail the proposed PQSM scheme, the rest of this paper is organized as follows. Section II describes the principle of PQSM and its implementation algorithm. Section III analyzes its performance, including the ABER performance and receiver complexity. The optimal number of antenna groups and order of signal constellation are determined in Section IV. Simulation results are presented and discussed in Section V and, finally, Section VI concludes the paper.

Notation: Throughout the paper, regular letters denote scalars while bold ones in lower- and upper-case represent vectors and matrices, respectively. The symbol $\mathbb{C}^{m\times n}$ means the complex space of $m \times n$ dimensions. The operators $\Re\{\cdot\}$ and $\Im\{\cdot\}$ take the real and imaginary parts of a complex variable, respectively. The $(i, j)^{\text{th}}$ entry of matrix $\boldsymbol{A}$ is denoted $\boldsymbol{A}_{i,j}$, and $(\cdot)^T$ and $(\cdot)^H$ refer to the transpose and Hermitian transpose, respectively. $\|\cdot\|$ means the Euclidean norm of

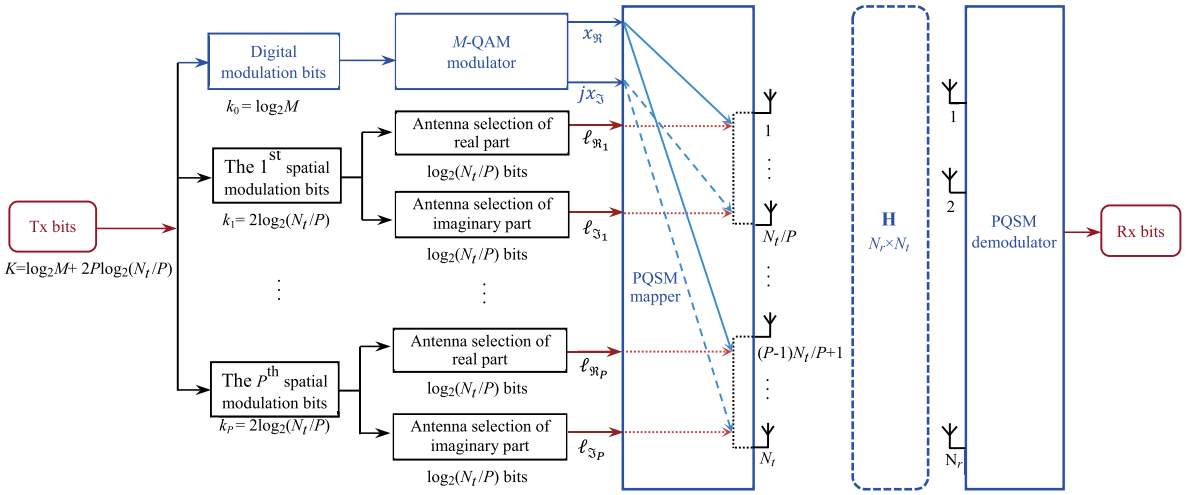

FIGURE 1. Principle of the proposed PQSM scheme.

a vector or the Frobenius norm of a matrix. The abbreviation $\mathcal{CN}(0, N_0)$ implies a complex Gaussian distribution with zero mean and variance N_0. Finally, the binomial coefficient and Gaussian Q-function are defined as $\binom{m}{n} \triangleq \frac{m!}{n!\,(m-n)!}$ and $Q(x) \triangleq \frac{1}{\sqrt{2\pi}} \int_x^\infty \exp\left(-\frac{1}{2}t^2\right) \mathrm{d}t$, respectively.

II. PQSM: PRINCIPLE AND IMPLEMENTATION

Consider an $N_r \times N_t$ MIMO system, with N_r and N_t being the number of receive (Rx) and Tx antennas, respectively. Also, N_t is assumed to be an even integer as a power of two. Suppose that the channels between the transmitter and the receiver are subject to block flat Rayleigh fading. In other words, the channel matrix $\boldsymbol{H} \in \mathbb{C}^{N_r \times N_t}$ keeps constant during a time slot, but varies independently between consecutive time slots. The $(m, n)^{\text{th}}$ entry of $\boldsymbol{H}$ refers to the channel coefficient from the n^{th} Tx antenna to the m^{th} Rx antenna, and all entries of $\boldsymbol{H}$ are independent and identically distributed (i.i.d.) circularly symmetric complex Gaussian random variables according to $\mathcal{CN}(0, 1)$.

Figure 1 illustrates the principle of the proposed PQSM scheme. At first, N_t Tx antennas are equally divided into P groups. Since one QSM, which occupies one or two Tx antennas, is applied in each antenna group, the maximum value of P is $N_t/2$. Thus, we have $2 \le P \le N_t/2$. For antennas in the i^{th} group, for all $i \in \{1, 2, \cdots, P\}$, they are indexed $n_i \in \{(i-1)\,N_t/P + 1, (i-1)N_t/P + 2, \cdots, i\,N_t/P\}$, as shown in Figure 1.

A. TRANSMITTER DESIGN

Assume M-QAM signal constellation is applied at the transmitter, with M being the order of signal constellation. In other words, the same M-QAM data symbol is sent to all the Tx antenna groups in a time slot. In PQSM scheme, P QSMs are performed in parallel in P groups of Tx antenna. Since $2\log_2 \widetilde{N}$ bits can be carried by the activated antenna indices in one QSM [7], P QSMs can carry $2P\log_2 \widetilde{N}$ bits in spatial domain, where $\widetilde{N} = N_t/P$ is the number of antenna in each antenna group. In addition, an M-QAM signal constellation symbol can carry $\log_2 M$ bits in signal domain. Therefore, in PQSM, the number of data bits to be transmitted during a time slot is

$$K = \log_2 M + 2P \log_2 \frac{N_t}{P}, \tag{1}$$

namely, the spectral efficiency of PQSM is K bits per channel use (bpcu). Then, the K bits are divided into $P + 1$ parts of length $k_0, k_1, \cdots, k_P$, with $k_0 = \log_2 M$ and $k_1 = k_2 = \cdots = k_P = 2\log_2 (N_t/P)$. Next, the operation of PQSM at the transmitter is described step-by-step.

1) The first k_0 bits are used to map a corresponding data symbol x out of the M-QAM constellation, given by

$$x = x_\Re + jx_\Im, \tag{2}$$

where $j = \sqrt{-1}$ is the imaginary unit. Then, the symbol x is processed by an inphase/quadrature (IQ)-modulation based RF chain, yielding

$$\begin{aligned} s(t) &= \Re\left\{xe^{-j2\pi f_c t}\right\} \\ &= x_\Re \cos(2\pi f_c t) + x_\Im \sin(2\pi f_c t), \end{aligned} \tag{3}$$

where f_c refers to the carrier frequency.

2) The intermediate k_1 bits are used for the first QSM. Specifically, the k_1 bits are equally divided into two subgroups of length $\log_2 (N_t/P)$, and each subgroup is applied to activate one antenna out of the first group of Tx antennas. Assume that the indices of the activated antennas are $\ell_{\Re_1}$ and $\ell_{\Im_1}$, it is evident that $\ell_{\Re_1}$, $\ell_{\Im_1} \in \{1, 2, \cdots, N_t/P\}$. Afterwards, $x_\Re$ and $x_\Im$ of the data symbol x are transmitted through antennas $\ell_{\Re_1}$ and $\ell_{\Im_1}$, respectively.

3) The subsequent k_i bits, for all $i \in \{2, 3, \cdots, P\}$, are used for the i^{th} QSM. Like the preceding step, the k_i bits are equally divided into two subgroups

of length $\log_2(N_t/P)$, and each subgroup is applied to activate one antenna out of the i^{th} group of Tx antennas. Assume that the indices of the chosen antennas are $\ell_{\Re_i}$ and $\ell_{\Im_i}$, where $\ell_{\Re_i}, \ell_{\Im_i} \in \{(i-1)N_t/P+1, (i-1)N_t/P+2, \cdots, iN_t/P\}$, then $x_\Re$ and $x_\Im$ in (3) are transmitted through the antennas $\ell_{\Re_i}$ and $\ell_{\Im_i}$, respectively.

As described in Section I, since one QSM activates one or two antennas, after performing P QSMs in parallel, the number of activated Tx antennas is between P and $2P$, and the number of selected Tx antenna indices used for carrying data bits is $2P$. Namely, the data symbol x is simultaneously transmitted through activated Tx antennas with indices $(\ell_{\Re_1}, \ell_{\Im_1}), \cdots, (\ell_{\Re_P}, \ell_{\Im_P})$.

Since more selected antenna indices can carry more data bits, for fixed spectral efficiency K and fixed number of Tx antennas N_t, larger P implies smaller M as per (1). In other words, by choosing different values of P, the proposed PQSM allows a tradeoff between the spatial domain and the signal domain. Clearly, lower signal constellation order enables larger Euclidean distance between constellation points, yielding lower ABER. Higher spatial modulation order, on the other hand, brings higher BER of spatial symbols detection. As a result, there exists a tradeoff between the spatial modulation order and the signal constellation order, whose optimal values will be determined in Section IV.

Now, the codeword to be transmitted is specified. On one hand, if $\ell_{\Re_i} \neq \ell_{\Im_i}$, for all $i \in \{1, 2, \cdots, P\}$, then the data bits transmitted by the activated antennas during a time slot form the codeword $\boldsymbol{w} \in \mathbb{C}^{N_t \times 1}$, which is of the form

$$\boldsymbol{w} = [\, \underset{}{0} \;\; \underset{\uparrow \ell_{\Re_1}}{x_\Re} \;\; \underset{}{0} \;\; \underset{\uparrow \ell_{\Im_1}}{jx_\Im} \;\; \underset{}{0} \;\; \underset{\uparrow \ell_{\Re_2}}{x_\Re} \;\; \underset{}{0} \;\; \underset{\uparrow \ell_{\Im_2}}{jx_\Im} \;\; \cdots \;\; \underset{}{0} \;\; \underset{\uparrow \ell_{\Re_P}}{x_\Re} \;\; \underset{}{0} \;\; \underset{\uparrow \ell_{\Im_P}}{jx_\Im} \;\; \underset{}{0} \,]^T, \tag{4}$$

where the antenna indices selected to transmit the data symbol are specified. It is clear from (4) that, except the rows with indices $\ell_{\Re_i}$ and $\ell_{\Im_i}$, for all $i \in \{1, 2, \cdots, P\}$, all elements in $\boldsymbol{w}$ are set to zero. On the other hand, if $\ell_{\Re_i} = \ell_{\Im_i} \triangleq \ell_i$, for all $i \in \{1, 2, \cdots, P\}$, namely, both the real and imaginary parts of data symbol x are transmitted through the same antenna with index ℓ_i in the i^{th} Tx antenna group. Accordingly, the ℓ_i^{th} element of codeword $\boldsymbol{w}$ shown in (4) becomes

$$w_{\ell_i} = x_\Re + jx_\Im. \tag{5}$$

No matter which case above occurs, ICI can be totally avoided since the carriers of $x_\Re$ and $x_\Im$ are orthogonal to each other. Finally, the modulated codeword with normalized Tx power is readily given by

$$\boldsymbol{s} = \frac{\boldsymbol{w}}{\|\boldsymbol{w}\|}. \tag{6}$$

To precisely illustrate the principle of the transmitter design based on the above discussions, the proposed PQSM transmission scheme is formalized in Algorithm 1. As an illustrative application, an example is shown below.

Algorithm 1 The Proposed PQSM Transmission Scheme

Require: N_t = number of Tx antennas, M = signal modulation order, P = number of antenna groups, and a random bit sequence $q = [b_1 b_2 \cdots b_K]$.

Ensure: The modulated codeword $\boldsymbol{s}$.

1: Initialization: $k_0 = \log_2 M$, $k_1 = \cdots = k_P = 2\log_2(N_t/P)$, and $\lambda \triangleq 2\log_2(N_t/P)$;
2: Divide the Tx antennas into P groups with indices $n_i \in \{(i-1)N_t/P+1, (i-1)N_t/P+2, \cdots, iN_t/P\}$, for all $i \in \{1, \cdots, P\}$;
3: Divide the bit sequence q into $P+1$ parts: $q_0 = [b_1 b_2 \cdots b_{k_0}]$ and $q_i = [b_{k_0+(i-1)\lambda+1}\, b_{k_0+(i-1)\lambda+2} \cdots b_{k_0+i\lambda}]$, for all $i \in \{1, \cdots, P\}$;
4: Map q_0 onto a M-QAM constellation symbol $x = x_\Re + jx_\Im$;
5: Subdivide q_i into two parts of equal length, by which the antenna indices $\ell_{\Re_i}$ and $\ell_{\Im_i}$ are determined, for all $i \in \{1, \cdots, P\}$;
6: With $\ell_{\Re_i}$ and $\ell_{\Im_i}$, for all $i \in \{1, \cdots, P\}$, the modulated codeword $\boldsymbol{s}$ is obtained as per (6).

Example: Consider a MIMO system with $N_t = 8$ Tx antennas and 4-QAM signal constellation applied, i.e., $M = 4$. In the case of $P = 2$, the Tx antennas are divided equally into two groups, with antenna indices $n_1 \in \{1, 2, 3, 4\}$ and $n_2 \in \{5, 6, 7, 8\}$. By virtue of (1), the block length (i.e., the spectral efficiency) can be calculated and given by $K = 10$, implying $k_0 = 2$ and $k_1 = k_2 = 4$. To be specific, assume the data sequence to be transmitted is

$$q = \begin{bmatrix} 0 & 1 & 1 & 1 & 0 & 1 & 1 & 0 & 1 & 0 \end{bmatrix}. \tag{7}$$

As per Algorithm 1, q can be divided into three parts:

$$q_0 = \begin{bmatrix} 0 & 1 \end{bmatrix},\ q_1 = \begin{bmatrix} 1 & 1 & 0 & 1 \end{bmatrix},\quad \text{and } q_2 = \begin{bmatrix} 1 & 0 & 1 & 0 \end{bmatrix}.$$

Then, q_0 is mapped onto the 4-QAM constellation, yielding $x = -1 + j$. Afterwards, q_1 is subdivided into two parts: [1 1] and [0 1], implying $\ell_{\Re_1} = 4$ and $\ell_{\Im_1} = 2$. Similarly, q_2 is subdivided into [1 0] and [1 0], yielding $\ell_{\Re_2} = \ell_{\Im_2} = 7$. As a result, according to (4), (5) and (6), the modulated codeword is given by

$$\boldsymbol{s} = \tfrac{1}{2}[\, 0 \;\; \underset{\uparrow 2}{j} \;\; 0 \;\; \underset{\uparrow 4}{-1} \;\; 0 \;\; 0 \;\; \underset{\uparrow (7,7)}{-1+j} \;\; 0 \,]^T, \tag{8}$$

where the activated antenna indices $(\ell_{\Re_1}, \ell_{\Im_1}) = (4, 2)$ and $(\ell_{\Re_2}, \ell_{\Im_2}) = (7, 7)$ are specified. Thus, after performing PQSM modulation, the bit sequence q is mapped onto a data symbol $x = -1 + j$, which is then transmitted through the activated antennas with indices (4, 2) and (7, 7).

Remark 1 (On the Data Symbol Transmitted in a Time Slot): In PQSM, the same data symbol is transmitted in parallel through the activated antennas in a time slot, yielding higher spatial diversity gain without ICI. On the contrary, if different symbols are transmitted in a time slot,

although the spectral efficiency can be further improved, it introduces ICI at the receiver, where advanced receiver like minimum mean squared error (MMSE) detector may have to be employed [21], [22]. As described in Section I, detection algorithms capable of reducing ICI in massive MIMO systems are very complicated, and high ICI would greatly degrade system performance.

B. DEMODULATION OF PQSM AT THE RECEIVER

At the receiver side, the received signal $\boldsymbol{y} \in \mathbb{C}^{N_r \times 1}$ can be expressed as

$$\boldsymbol{y} = \boldsymbol{H}\boldsymbol{s} + \boldsymbol{n}, \tag{9}$$

where $\boldsymbol{n} \in \mathbb{C}^{N_r \times 1}$ represents the additive white Gaussian noise (AWGN) with entries subject to i.i.d. $\mathcal{CN}(0, N_0)$. As the transmit power of codeword $\boldsymbol{s}$ is normalized to unity, the average signal-to-noise ratio (SNR) at the receiver is defined as $\rho \triangleq 1/N_0$.

Recalling Eq. (4) where $\ell_{\Re_i}$ and $\ell_{\Im_i}$ denote the activated antenna indices at the i^{th} Tx antenna group, let $\boldsymbol{h}_{\ell_{\Re_i}}$ and $\boldsymbol{h}_{\ell_{\Im_i}}$ be the $\ell_{\Re_i}^{\text{th}}$ and $\ell_{\Im_i}^{\text{th}}$ columns of $\boldsymbol{H}$, i.e.,

$$\begin{cases} \boldsymbol{h}_{\ell_{\Re_i}} = \left[h_{1,\ell_{\Re_i}}, h_{2,\ell_{\Re_i}}, \cdots, h_{N_r,\ell_{\Re_i}}\right]^T \\ \boldsymbol{h}_{\ell_{\Im_i}} = \left[h_{1,\ell_{\Im_i}}, h_{2,\ell_{\Im_i}}, \cdots, h_{N_r,\ell_{\Im_i}}\right]^T \end{cases}, \tag{10}$$

where $i \in \{1, 2, \cdots, P\}$. Moreover, since only P pairs of antenna indices are selected for data transmission, (9) can be rewritten as

$$\boldsymbol{y} = \sum_{i=1}^{P} \boldsymbol{h}_{\ell_{\Re_i}} x_{\Re} + j \sum_{i=1}^{P} \boldsymbol{h}_{\ell_{\Im_i}} x_{\Im} + \boldsymbol{n} = \boldsymbol{g} + \boldsymbol{n}, \tag{11}$$

where

$$\boldsymbol{g} \triangleq \sum_{i=1}^{P} \boldsymbol{h}_{\ell_{\Re_i}} x_{\Re} + j \sum_{i=1}^{P} \boldsymbol{h}_{\ell_{\Im_i}} x_{\Im}. \tag{12}$$

Assume that channel state information (CSI) is perfectly known and the optimum maximum likelihood (ML) detector is exploited at the receiver. Accordingly, the estimated antenna indices and transmitted data symbols are readily given by

$$\begin{aligned} \left[\hat{\boldsymbol{\ell}}_{\Re}, \hat{\boldsymbol{\ell}}_{\Im}, \hat{x}_{\Re}, \hat{x}_{\Im}\right] &= \arg \min_{\boldsymbol{\ell}_{\Re}, \boldsymbol{\ell}_{\Im}, x_{\Re}, x_{\Im}} \|\boldsymbol{y} - \boldsymbol{g}\|^2 \\ &= \arg \min_{\boldsymbol{\ell}_{\Re}, \boldsymbol{\ell}_{\Im}, x_{\Re}, x_{\Im}} \|\boldsymbol{g}\|^2 - 2\,\Re\{\boldsymbol{y}^H \boldsymbol{g}\}, \end{aligned} \tag{13}$$

where

$$\hat{\boldsymbol{\ell}}_{\Re} = (\hat{\ell}_{\Re_1}, \hat{\ell}_{\Re_2}, \cdots, \hat{\ell}_{\Re_P}), \tag{14a}$$
$$\hat{\boldsymbol{\ell}}_{\Im} = (\hat{\ell}_{\Im_1}, \hat{\ell}_{\Im_2}, \cdots, \hat{\ell}_{\Im_P}), \tag{14b}$$
$$\boldsymbol{\ell}_{\Re} = (\ell_{\Re_1}, \ell_{\Re_2}, \cdots, \ell_{\Re_P}), \tag{14c}$$

and

$$\boldsymbol{\ell}_{\Im} = (\ell_{\Im_1}, \ell_{\Im_2}, \cdots, \ell_{\Im_P}). \tag{14d}$$

III. PERFORMANCE AND COMPLEXITY ANALYSES

In this section, an upper bound on the ABER of PQSM is first derived and, then, the receiver complexity is quantified and compared with those of GSM and QSM.

A. BIT ERROR RATE ANALYSIS

Now, we analyze the ABER performance of PQSM by using the well-known union bound technique [23, pp. 263-264].

Specifically, with the optimum ML detector given by (13), the union bound on the ABER can be given by

$$\bar{P}_{\text{E}} \leq \frac{1}{K\,2^K} \sum_{n=1}^{2^K} \sum_{m=1}^{2^K} \bar{P}_{\text{APEP}}\left(\boldsymbol{s}_n \to \hat{\boldsymbol{s}}_m\right) e_{n,m}, \tag{15}$$

where $\bar{P}_{\text{APEP}}\left(\boldsymbol{s}_n \to \hat{\boldsymbol{s}}_m\right)$ denotes the *average* pairwise error probability (APEP) given that the codeword $\boldsymbol{s}_n$ is transmitted whereas the estimated codeword at the receiver is $\hat{\boldsymbol{s}}_m$, and $e_{n,m}$ is the total number of erroneous bits pertaining to the pairwise error event $\boldsymbol{s}_n \to \hat{\boldsymbol{s}}_m$, i.e., the Hamming distance of codeword $\boldsymbol{s}_n$ and $\hat{\boldsymbol{s}}_m$.

To calculate the APEP needed in (15), we first derive the *instantaneous* pairwise error probability. To be specific, in case $\boldsymbol{s}$ is transmitted whereas it is incorrectly decoded as $\hat{\boldsymbol{s}}$, the instantaneous pairwise error probability given the CSI $\boldsymbol{H}$, can be written as

$$\Pr\left(\boldsymbol{s} \to \hat{\boldsymbol{s}} | \boldsymbol{H}\right) = \Pr\left(\boldsymbol{g} \to \hat{\boldsymbol{g}} | \boldsymbol{H}\right) = Q\left(\sqrt{\mu}\right), \tag{16}$$

where $\boldsymbol{g}$ was earlier defined in (12), and

$$\hat{\boldsymbol{g}} \triangleq \sum_{i=1}^{P} \hat{\boldsymbol{h}}_{\ell_{\Re_i}} \hat{x}_{\Re} + j \sum_{i=1}^{P} \hat{\boldsymbol{h}}_{\ell_{\Im_i}} \hat{x}_{\Im}, \tag{17}$$

$$\mu \triangleq \frac{1}{2N_0} \|\boldsymbol{g} - \hat{\boldsymbol{g}}\|^2 = \sum_{n=1}^{2N_r} \alpha_n^2, \tag{18}$$

with $\alpha_n \sim \mathcal{CN}(0, \sigma^2)$ referring to the channel estimation error, for all $n \in [1, 2N_r]$. The parameter μ defined in (18) is of Chi-squared distribution with $2N_r$ degrees of freedom, i.e., its PDF is expressed as

$$f_\mu(x) = \frac{1}{\sqrt{2\pi x}\,\sigma} e^{-\frac{x}{2\sigma^2}}, \; x \geq 0, \tag{19}$$

where

$$\sigma^2 = \frac{\rho}{2} \sum_{i=1}^{P} \beta_i, \tag{20}$$

with β_i given by (21), as shown at the bottom of the next page [7].

With (16) and (19), the APEP needed in (15) can been computed as

$$\bar{P}_{\text{APEP}}\left(\boldsymbol{s}_n \to \hat{\boldsymbol{s}}_m\right) = \int_0^\infty Q\left(\sqrt{x}\right) f_\mu(x)\,\mathrm{d}x. \tag{22}$$

After some calculus operations, (22) can be written in the closed-form:

$$\begin{aligned} &\bar{P}_{\text{APEP}}\left(\boldsymbol{s}_n \to \hat{\boldsymbol{s}}_m\right) \\ &= \left(\frac{1-\gamma}{2}\right)^{N_r} \sum_{i=0}^{N_r-1} \binom{N_r - 1 + i}{i} \left(\frac{1+\gamma}{2}\right)^i, \end{aligned} \tag{23}$$

where $\gamma \triangleq \sqrt{\frac{\sigma^2}{2+\sigma^2}}$. Moreover, performing Taylor series expansion over (23) and ignoring higher order terms, (23) can be approximated as

$$\bar{P}_{\text{APEP}}\left(\boldsymbol{s}_n \to \hat{\boldsymbol{s}}_m\right) \approx \frac{2^{N_r-1}\Gamma(N_r+0.5)}{\sqrt{\pi(N_r)!}}\left(\frac{1}{\sigma^2}\right)^{N_r}. \quad (24)$$

Finally, substituting (23) into (15) yields the union upper-bound on ABER, explicitly shown in (25), as shown at the bottom of this page.

B. RECEIVER COMPLEXITY ANALYSIS

In this subsection, the computational complexity of the optimum ML detector discussed in Section II-B is quantified, and compared with those of GSM and QSM. In particular, both the number of complex multiplications and additions are accounted for in the following calculation.

For the proposed PQSM scheme, as per (12)-(13), the complexity emanates from:

i) computing $\boldsymbol{g}$, which requires $(4P-1)N_r$ complex operations;
ii) computing $\|\boldsymbol{y}-\boldsymbol{g}\|^2$, which requires $3N_r-1$ complex operations;
iii) repeating the above operations $M(N_t/P)^{2P}$ times.

To sum up, the computational complexity of the optimum ML receiver of PQSM is given by

$$\eta_1 = (4PN_r + 2N_r - 1)2^K. \quad (26)$$

As far as QSM is concerned, according to [7, Eq. (3)], the complexity of ML detector is the result of

i) computing $\boldsymbol{g}$, which requires $3N_r$ complex operations;
ii) computing $\|\boldsymbol{y}-\boldsymbol{g}\|^2$, which requires $3N_r-1$ operations;
iii) repeating the above operations $M'N_t{}^2$ times, where M' is the signal constellation order of QSM.

Thus, the receiver complexity of QSM is given by

$$\eta_2 = (6N_r - 1)\,2^{K'}, \quad (27)$$

where

$$K' = \log_2 M' + 2\log_2 N_t \quad (28)$$

is the spectral efficiency of QSM in bpcu [7].

When PQSM and QSM are applied to the same MIMO system, if their orders of signal constellation are identical (i.e., $M = M'$), comparing (1) with (28) one can conclude that PQSM has higher spectral efficiency (i.e., $K > K'$ for all $P \geq 2$) but at the cost of ABER. Therefore, the receiver complexity of the two schemes is not comparable in this case. For a fair comparison, assume that both schemes have the same spectral efficiency, i.e., $K = K'$, which implies $M < M'$, then by virtue of (26) and (27), the receiver complexity ratio of PQSM to QSM is

$$R = \frac{\eta_1}{\eta_2} = \frac{4PN_r + 2N_r - 1}{6N_r - 1}, \quad (29)$$

which equals unity if $P = 1$, and approximates $(2P+1)/3$ if $P > 1$. It is not surprising that $R = 1$ if $P = 1$, since in such a case the proposed PQSM reduces to the conventional QSM. On the other hand, if $P > 1$, it is clear that the computational complexity of PQSM is linearly proportional to P, i.e., the number of Tx antenna groups. This is indeed the cost of the ABER gain obtained by PQSM, as illustrated in Section V.

TABLE 1. Comparison of receiver complexity.

Modulation Scheme	Number of Activated Antennas	Receiver Complexity
PQSM	$P \sim 2P$	$\mathcal{O}(PN_PM)$
QSM	1 or 2	$\mathcal{O}(N_t^2M')$
GSM	N_u	$\mathcal{O}(N_uN_c'M'')$

The receiver complexity of GSM can be computed by using a similar approach as in [5]. For comparison purpose, the receiver complexities of PQSM, QSM and GSM are summarized in Table 1, where $N_P = (N_t/P)^{2P}$, and $N_c' = 2^{\lfloor \log_2 \binom{N_t}{N_u} \rfloor}$ with N_u being the number of active antennas in GSM. The parameters M, M' and M'' refer to the orders of signal constellation applied to PQSM, QSM and GSM, respectively.

It is noteworthy that the receiver complexity in PQSM can be readily reduced because there are many zeros in the transmission vector as shown in (4). Moreover, since the same data symbol is transmitted in parallel by multiple activated Tx antennas, there is no ICI and, thus, the receiver complexity can be further reduced. For more details on receiver complexity reduction, the interested reader is referred to [24], [25].

$$\beta_i = \begin{cases} |x_\Re|^2 + |\hat{x}_\Re|^2 + |x_\Im|^2 + |\hat{x}_\Im|^2, & \text{if } \boldsymbol{h}_{\ell_{\Re_i}} \neq \hat{\boldsymbol{h}}_{\ell_{\Re_i}} \text{ and } \boldsymbol{h}_{\ell_{\Im_i}} \neq \hat{\boldsymbol{h}}_{\ell_{\Im_i}} \\ |x_\Re - \hat{x}_\Re|^2 + |x_\Im|^2 + |\hat{x}_\Im|^2, & \text{if } \boldsymbol{h}_{\ell_{\Re_i}} = \hat{\boldsymbol{h}}_{\ell_{\Re_i}} \text{ and } \boldsymbol{h}_{\ell_{\Im_i}} \neq \hat{\boldsymbol{h}}_{\ell_{\Im_i}} \\ |x_\Re|^2 + |\hat{x}_\Re|^2 + |x_\Im - \hat{x}_\Im|^2, & \text{if } \boldsymbol{h}_{\ell_{\Re_i}} \neq \hat{\boldsymbol{h}}_{\ell_{\Re_i}} \text{ and } \boldsymbol{h}_{\ell_{\Im_i}} = \hat{\boldsymbol{h}}_{\ell_{\Im_i}} \\ |x_\Re - \hat{x}_\Re|^2 + |x_\Im - \hat{x}_\Im|^2, & \text{if } \boldsymbol{h}_{\ell_{\Re_i}} = \hat{\boldsymbol{h}}_{\ell_{\Re_i}} \text{ and } \boldsymbol{h}_{\ell_{\Im_i}} = \hat{\boldsymbol{h}}_{\ell_{\Im_i}} \end{cases} \quad (21)$$

$$\bar{P}_{\text{E}} \leq \frac{1}{K\,2^K}\sum_{n=1}^{2^K}\sum_{m=1}^{2^K}\left[e_{n,m}\left(\frac{1-\gamma}{2}\right)^{N_r}\sum_{i=0}^{N_r-1}\binom{N_r-1+i}{i}\left(\frac{1+\gamma}{2}\right)^{i}\right]. \quad (25)$$

IV. OPTIMAL NUMBER OF ANTENNA GROUPS AND SIGNAL CONSTELLATION ORDER

Since PQSM allows a tradeoff between the spatial domain and the signal constellation domain, in this section the optimal number of Tx antenna groups and order of signal constellation, denoted by P_{opt} and M_{opt} respectively, are determined so as to minimize ABER. Specifically, the optimization problem can be formulated as

$$(P_{\text{opt}}, M_{\text{opt}}) = \arg\min_{P,\,M} \bar{P}_{\text{E}} \tag{30a}$$

$$\text{s.t. } 2 \le P \le \frac{N_t}{2}, \tag{30b}$$

$$\log_2 M + 2P \log_2 \frac{N_t}{P} = K, \tag{30c}$$

$$\frac{N_t}{P} \text{ is an integer as a power of 2.} \tag{30d}$$

Although this is a complex discrete variable optimization problem, it can be readily solved by means of simple searching, since the number of feasible parameter pairs (P, M) is not large. For instance, consider a MIMO system with $(N_t, N_r) = (16, 16)$ and $K = 18$. According to Eqs. (30b)-(30d), the set of feasible parameter pairs (P, M) can be explicitly given by $\{(2, 64), (4, 4), (8, 4)\}$, which has only three possibilities. As a result, the values of P_{opt} and M_{opt} can be readily determined via a searching algorithm.

In a real-world MIMO system, the ABER must be less than a predefined threshold, denoted by E_{th}, that is, an additional constraint is

$$\bar{P}_{\text{E}} \le E_{\text{th}}. \tag{31}$$

Given N_t, N_r and K, it is clear that the upper bound on ABER, i.e., (25), depends upon SNR. Thus, for any feasible parameter pair (P, M), we need an appropriate SNR to satisfy (31). According to (15), (20) and (24), it is not hard to find that the ABER is a monotonically decreasing function of ρ. Thus, by choosing an appropriate ρ, Eq. (31) can always be satisfied.

Accounting for all the above concerns, a search algorithm to determine the values of P_{opt} and M_{opt} is formalized in Algorithm 2. As an illustrative example, consider a MIMO system with $(N_t, N_r) = (8, 8)$ and $K = 12$, it is not hard to find that the possible set of feasible parameter pairs is $\{(2, 16), (4, 16)\}$. By using Algorithm 2, we can readily obtain the optimal parameter pair $(P_{\text{opt}}, M_{\text{opt}}) = (2, 16)$.

Compared with the conventional QSM scheme, the proposed PQSM scheme with the optimal values of P_{opt} and M_{opt} offers the best tradeoff between the spatial domain and the signal constellation domain, which enables to minimize the ABER without loss of spectral efficiency, thus improving the system reliability. The performance of Algorithm 2 will be illustrated in Subsection V-C.

Remark 2 (On the Value of $\Delta\rho$ in Step 5 of Algorithm 2): For a given MIMO system and target spectral efficiency, the goal of Algorithm 2 is to find the optimal number of Tx antenna groups and optimal signal constellation order

Algorithm 2 Optimal Number of Tx Antenna Groups and Order of Signal Constellation

Require: N_t = number of Tx antennas, N_r = number of Rx antennas, K = target spectral efficiency, and E_{th} = threshold of ABER.

Ensure: $(P_{\text{opt}}, M_{\text{opt}})$ {The optimal number of Tx antenna groups and the optimal order of signal constellation}.

1: List the set of all the feasible parameter pairs $\{(P_1, M_1), \cdots, (P_n, M_n)\}$ as per (30b)-(30d), where n is the number of feasible parameter pairs;
2: Set the initial SNR $\rho = 0$ (in the unit of dB) and the initial ABER vector $\boldsymbol{P}_{\text{E}} = [\bar{P}_{\text{E}_1}, \bar{P}_{\text{E}_2}, \cdots, \bar{P}_{\text{E}_n}] = [1, 1, \cdots, 1]$, where $\bar{P}_{\text{E}_i}$ is the initial ABER corresponding to feasible parameter pair (P_i, M_i), for all $i \in \{1, \cdots, n\}$;
3: Set $P_0 = \min(\boldsymbol{P}_{\text{E}})$;
4: **while** $P_0 > E_{\text{th}}$ **do**
5: $\quad\rho = \rho + \Delta\rho$, where $\Delta\rho$ denotes the SNR increment;
6: $\quad$**for** $i = 1 : n$ **do**
7: $\quad\quad$Compute $\bar{P}_{\text{E}_i}$ corresponding to feasible parameter pair (P_i, M_i) according to (25);
8: $\quad$**end for**
9: $\quad$Update $P_0 = \min(\boldsymbol{P}_{\text{E}})$;
10: $\quad$Identify k as the index of the smallest entry in $\boldsymbol{P}_{\text{E}}$;
11: **end while**
12: $(P_{\text{opt}}, M_{\text{opt}}) = (P_k, M_k)$.

achieving the best tradeoff between the spatial domain and the signal domain, such that the ABER of the MIMO system is minimized. On one hand, for each feasible parameter pair (P_i, M_i), where $i \in [1, n]$ with n being the number of feasible parameter pairs, Algorithm 2 calculates the ABER vector $\boldsymbol{P}_{\text{E}} = [\bar{P}_{\text{E}_1}, \bar{P}_{\text{E}_2}, \cdots, \bar{P}_{\text{E}_n}]$ under a certain SNR ρ, where $\bar{P}_{\text{E}_i}$ is the ABER corresponding to feasible parameter pair (P_i, M_i). By gradually increasing ρ until at least one entry of vector $\boldsymbol{P}_{\text{E}}$ is less than or equal to E_{th}, and assume the smallest entry in vector $\boldsymbol{P}_{\text{E}}$ at this time is $\bar{P}_{\text{E}_k}$, namely, $\bar{P}_{\text{E}_k} = \min(\bar{P}_{\text{E}_1}, \bar{P}_{\text{E}_2}, \cdots, \bar{P}_{\text{E}_n})$. Then, (P_k, M_k) is the optimal feasible parameter pair $(P_{\text{opt}}, M_{\text{opt}})$. In other words, in the process of gradually increasing ρ, the feasible parameter pair (P_k, M_k) that first satisfy $\bar{P}_{\text{E}_k} \le E_{\text{th}}$ is taken as the optimal parameter pair. On the other hand, according to (15), (20) and (24), it is evident that ABER monotonically decreases as ρ increases. As a result, (31) can be satisfied as long as ρ is sufficiently large. In other words, $\Delta\rho$ can be as large as possible to find the optimal solution quickly. Consequently, in our simulation experiments to be discussed next, $\Delta\rho$ is set to unity.

V. SIMULATION RESULTS AND DISCUSSIONS

In this section, Monte-Carlo simulation results pertaining to the proposed PQSM scheme with different Tx antenna groups and signal constellation orders are presented and compared with the conventional QSM [7] and GSM [5] schemes.

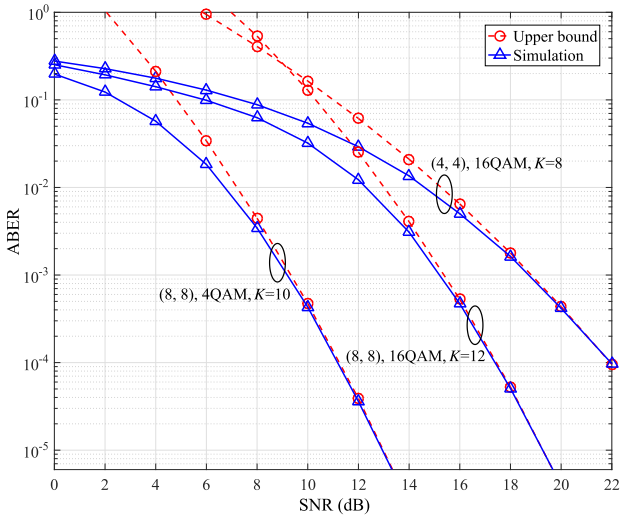

FIGURE 2. The ABER of PQSM ($P = 2$) versus SNR for different antenna configurations and various signal constellation orders.

For each Monte-Carlo realization, at least 10^6 symbols are transmitted to obtain the ABER for each SNR value, and the transmission energy E_s is normalized to unity.

A. THE TIGHTNESS OF THE ABER UPPER-BOUND GIVEN BY EQ. (25)

Figure 2 shows the ABER of PQSM with $P = 2$ versus SNR in the unit of dB, where three scenarios are considered, namely, $(N_t, N_r) = (4, 4)$ with 16-QAM, $(N_t, N_r) = (8, 8)$ with 16-QAM, and 4-QAM. For each scenario, the simulation results are compared with the upper-bound computed as per (25). It is observed that, for each scenario, the upper-bound is very tight with corresponding simulation result at high SNR, which corroborates the effectiveness of our preceding analysis. Moreover, if the signal constellation is fixed to 16-QAM, the ABER decreases significantly as the number of antennas increases from $(4, 4)$ to $(8, 8)$, due to larger Rx *diversity gain*, corresponding to the steeper slope of the latter curve than the former in the figure. On the other hand, if the antenna configuration is fixed to $(N_t, N_r) = (8, 8)$, the ABER decreases significantly when the signal constellation changes from 16-QAM to 4-QAM, since the latter has larger Euclidean distance between signal constellation points. This is widely known as *coding gain*, corresponding to the horizontal shift of the latter curve relative to the former.

B. COMPARISON OF PQSM AND QSM

As discussed earlier, the spectral efficiency of PQSM is $K = \log_2 M + 2P \log_2(N_t/P)$ while that of QSM is $K' = \log_2 M' + 2 \log_2 N_t$. If the same order of signal constellation is applied, i.e., $M = M'$, the spectral efficiency of PQSM is clearly higher than QSM, as shown in Table 2. In the following, to guarantee the fairness of performance comparison, both PQSM and QSM use M-QAM

TABLE 2. Comparison of spectral efficiency between PQSM and QSM using the same 4-QAM constellation.

Spectral Efficiency (bpcu)	Number of Tx Antennas				
	8	16	32	64	128
QSM	8	10	12	14	16
PQSM, $P = 2$	10	14	18	22	26
PQSM, $P = 4$	10	18	26	34	42

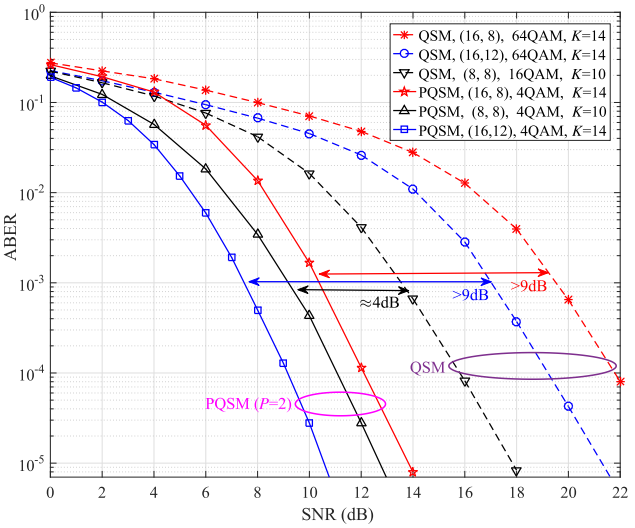

FIGURE 3. The ABER comparison between PQSM ($P = 2$) and QSM, with $(N_t, N_r) = (8, 8)$, $(16, 8)$, $(16, 12)$ and $K = 10, 14, 14$, respectively.

constellation with appropriate orders of spatial modulation and signal constellation, such that they achieve the same target spectral efficiency.

In Figure 3, the ABER performance of PQSM and QSM are compared, where $(N_t, N_r) = (8, 8)$, $(16, 8)$ and $(16, 12)$, and $K = 10$, 14 and 14 are considered, respectively. The number of Tx antenna groups of PQSM is fixed to $P = 2$. As seen from the figure, for each scenario, PQSM has lower ABER than that of QSM in the whole SNR region under consideration. This is because in the PQSM scheme two pairs of Tx antenna indices are selected in a time slot, which reduces the signal constellation order by mapping more bits to the spatial domain than to the signal domain. This decrease in signal constellation order leads to larger Euclidean distance between constellation points, thus yielding lower ABER.

Figure 3 also illustrates that, compared with QSM, the ABER improvement of PQSM is more significant when the number of Tx antennas becomes larger. In particular, if the ABER is set to 10^{-3}, it is observed from the figure that PQSM has about 4 dB SNR gain over QSM in the case of $N_t = 8$, while the gain is larger than 9 dB when $N_t = 16$. The significant SNR gain is mainly due to the fact that the PQSM scheme requires a lower signal constellation order to achieve the same spectral efficiency as QSM when the number of

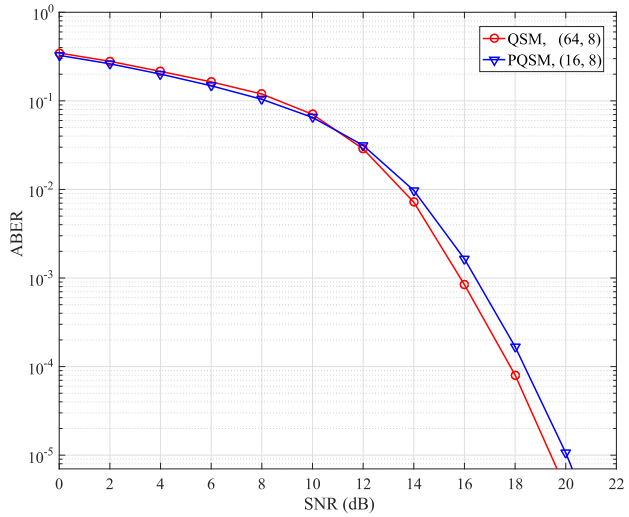

FIGURE 4. The ABER comparison between PQSM ($P = 2$) with $(N_t, N_r) = (16, 8)$ and QSM with $(N_t, N_r) = (64, 8)$, in the same context of $K = 16$ and 16-QAM.

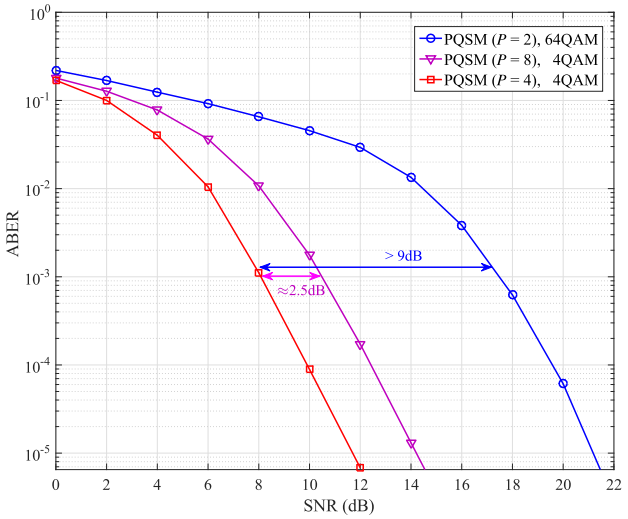

FIGURE 5. The ABER of PQSM ($P = 2, 4, 8$) in the same context of $(N_t, N_r) = (16, 16)$ and $K = 18$.

Tx antennas increases. Consequently, PQSM is more suitable than QSM for massive MIMO systems.

In Figure 4, the ABER performance of PQSM with $P = 2$ and QSM schemes under the same constellation order $M = 16$, is compared. To achieve the same spectral efficiency $K = K' = 16$ bpcu, the PQSM scheme needs $N_t = 16$ whereas QSM requires $N_t = 64$. This means that, given a particular signal constellation order, PQSM can achieve the same spectral efficiency as QSM but with much less Tx antennas. In such a case, Figure 4 shows that the ABER performance of PQSM is almost the same as that of QSM at low SNR, yet slightly worse at high SNR. The reason behind this observation is that the ABER is dominated by the signal constellation symbols at low SNR whereas by the spatial symbols at high SNR [3]. This figure demonstrates that, for the same spectral efficiency and similar ABER, PSQM needs much less Tx antennas than QSM, which greatly reduces the hardware cost in practice.

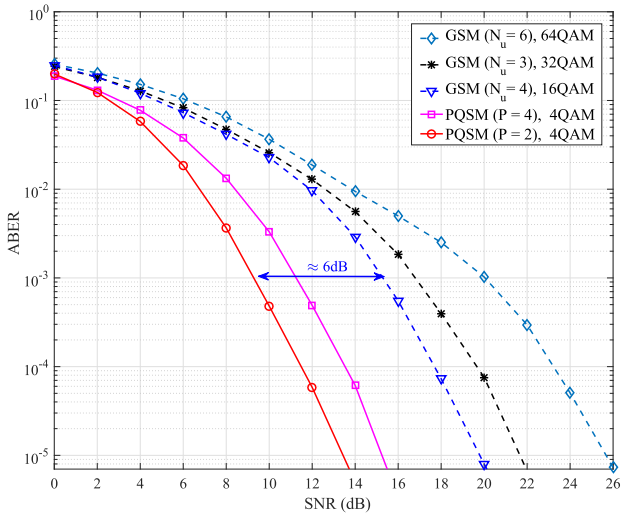

FIGURE 6. The ABER comparison between PQSM ($P = 2, 4$) and GSM ($N_u = 3, 4, 6$), in the same context of $(N_t, N_r) = (8, 8)$ and $K = 10$.

C. OPTIMAL NUMBER OF TX ANTENNA GROUPS AND ORDER OF SIGNAL CONSTELLATION

To validate the performance of Algorithm 2 for PQSM, Figure 5 depicts the ABER performance of PQSM for different (P, M) pairs, with $(N_t, N_r) = (16, 16)$ and $K = 18$ bpcu. For the MIMO system with $(N_t, N_r) = (16, 16)$ and the target spectral efficiency $K = 18$ bpcu, the set of all (P, M) feasible pairs is $\{(2, 64), (4, 4), (8, 4)\}$. According to Algorithm 2, it is not hard to determine that the optimal parameters are $(P_{\text{opt}}, M_{\text{opt}}) = (4, 4)$. As can be seen from Figure 5, the case with $(P, M) = (P_{\text{opt}}, M_{\text{opt}}) = (4, 4)$ outperforms the others, since it achieves the best tradeoff between spatial modulation order and signal constellation order. On one hand, for the scenarios of PQSM ($P = 2$) with 64QAM and PQSM ($P = 4$) with 4QAM, the latter has larger Euclidean distance between signal constellation points, thus yielding lower ABER. On the other hand, for the scenarios with $P = 8$ and $P = 4$, although both of them have the same spectral efficiency and the order of signal constellation. However, the latter has lower BER of spatial symbols detection than the former. Consequently, the case of $P = 4$ has lower ABER than the case of $P = 8$. To be specific, if the ABER is set to 10^{-3}, Figure 5 shows that the case with $(P, M) = (P_{\text{opt}}, M_{\text{opt}}) = (4, 4)$ has about 9 dB SNR gain over the case with $(P, M) = (2, 64)$, and 2.5 dB gain over the case with $(P, M) = (8, 4)$.

D. COMPARISON OF PQSM AND GSM

Figure 6 compares the ABER performance of PQSM with $(P, M) = (2, 4), (4, 4)$ and GSM with $(N_u, M) = (3, 32), (4, 16), (6, 64)$, where $(N_t, N_r) = (8, 8)$, $K = 10$ bpcu, and N_u denotes the number of active antennas in GSM. As observed from the figure, both PQSM schemes have lower ABER than that of GSM schemes. This is because, to achieve

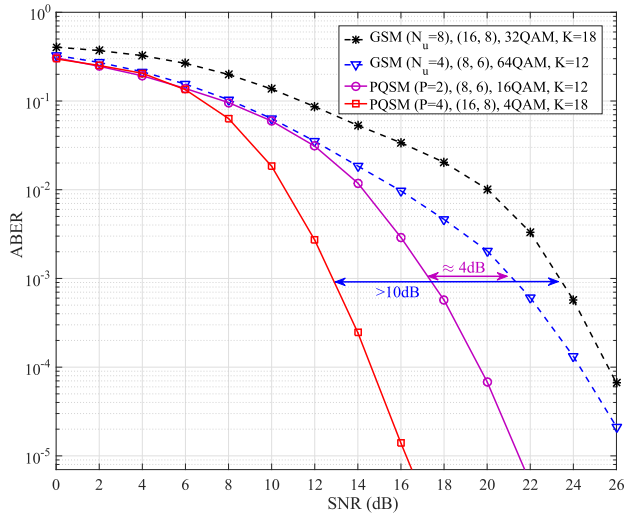

FIGURE 7. The ABER performance comparison between PQSM ($P = 2, 4$) and GSM ($N_u = 4, 8$).

the same target spectral efficiency, PQSM uses a lower order of signal constellation than that of GSM, thus yielding lower ABER. It can also be seen from Figure 6 that the ABER performance of PQSM ($P = 2$) outperforms that of PQSM ($P = 4$). In other words, using more Tx antenna groups does not necessarily lead to lower ABER. Accordingly, Algorithm 2 can be exploited to find the optimal number of Tx antenna groups and the optimal order of signal constellation, given by $(P_{\text{opt}}, M_{\text{opt}}) = (2, 4)$, which is in agreement with the simulation results shown in Figure 6.

Figure 7 compares the ABER of PQSM and GSM, where two scenarios, namely, $(N_t, N_r) = (8, 6)$ and $(16, 8)$, and $K = 12$ and 18, are considered, respectively. For the cases of $(N_t, N_r) = (8, 6)$ with $K = 12$ and $(N_t, N_r) = (16, 8)$ with $K = 18$, according to Algorithm 2, it is not hard to find the optimal parameters are $(P_{\text{opt}}, M_{\text{opt}}) = (2, 16)$ and $(4, 4)$, respectively, as depicted in Figure 7. For each case, PQSM and GSM use the same number of maximum activated antennas. Figure 7 shows that, for the same spectral efficiency, PQSM outperforms GSM in terms of ABER. Specifically, if the ABER is set to 10^{-3}, for the case with $(N_t, N_r) = (16, 8)$, the PQSM scheme with $(P, M) = (4, 4)$ has about 10 dB SNR gain over the GSM scheme with $(N_u, M) = (8, 32)$, while for the case $(N_t, N_r) = (8, 6)$ the PQSM scheme with $(P, M) = (2, 16)$ has about 4 dB SNR gain over the GSM with $(N_u, M) = (4, 64)$. The reason behind this performance gain is that PQSM can map more information bits to the spatial domain and use a lower order of signal constellation, achieving a tradeoff between the spatial modulation order and the signal constellation order.

VI. CONCLUDING REMARKS

To achieve higher spectral efficiency and/or reliability in massive MIMO systems while avoiding ICI, a PQSM scheme was proposed in this paper, which includes the conventional QSM as a special case. The distinctive feature of the PQSM technique is to allow a tradeoff between spatial modulation order and signal constellation order. On one hand, for a fixed order of signal constellation, PQSM can achieve higher spectral efficiency with higher spatial modulation order, or maintain the spectral efficiency but using much less Tx antennas. On the other hand, by choosing the optimal number of Tx antenna groups, PQSM can significantly decrease ABER without loss of spectral efficiency. Furthermore, PQSM can completely avoid ICI and ISI. Besides the implementation algorithm of PQSM and the corresponding ABER analysis, an optimization algorithm was designed to find the optimal number of Tx antenna groups and optimal order of signal constellation. Thanks to its flexibility and superiority over conventional QSM and GSM, the proposed PQSM is more suitable for massive MIMO promising in 5G wireless communication systems.

REFERENCES

[1] P. Patcharamaneepakorn, S. Wu, C.-X. Wang, E.-M. Aggoune, M. M. Alwakeel, X. Ge, and M. D. Renzo, "Spectral, energy, and economic efficiency of 5G multicell massive MIMO systems with generalized spatial modulation," *IEEE Trans. Veh. Technol.*, vol. 65, no. 12, pp. 9715–9730, Dec. 2016.

[2] Z. Yigit and E. Basar, "Double spatial modulation: A high-rate index modulation scheme for MIMO systems," in *Proc. Int. Sym. Wireless Commun. Syst. (ISWCS)*, Poznan, Poland, Sep. 2016, pp. 347–351.

[3] R. Y. Mesleh, H. Haas, S. Sinanovic, C. W. Ahn, and S. Yun, "Spatial modulation," *IEEE Trans. Veh. Technol.*, vol. 57, no. 4, pp. 2228–2241, Jul. 2008.

[4] M. Di Renzo, H. Haas, A. Ghrayeb, S. Sugiura, and L. Hanzo, "Spatial modulation for generalized MIMO: Challenges, opportunities, and implementation," *Proc. IEEE*, vol. 102, no. 1, pp. 56–103, Jan. 2014.

[5] A. Younis, N. Serafimovski, R. Mesleh, and H. Haas, "Generalised spatial modulation," in *Proc. 44th Asilomar Conf. Signals, Syst. Comput.*, Pacific Grove, CA, USA, Nov. 2010, pp. 1498–1502.

[6] J. Fu, C. Hou, W. Xiang, L. Yan, and Y. Hou, "Generalised spatial modulation with multiple active transmit antennas," in *Proc. IEEE Globecom Workshops*, Miami, FL, USA, Dec. 2010, pp. 839–844.

[7] R. Mesleh, S. S. Ikki, and H. M. Aggoune, "Quadrature spatial modulation," *IEEE Trans. Veh. Technol.*, vol. 64, no. 6, pp. 2738–2742, Jun. 2015.

[8] J. Li, M. Wen, X. Cheng, Y. Yan, S. Song, and M. H. Lee, "Generalized precoding-aided quadrature spatial modulation," *IEEE Trans. Veh. Technol.*, vol. 66, no. 2, pp. 1881–1886, Feb. 2017.

[9] Z. Yigit and E. Basar, "Low-complexity detection of quadrature spatial modulation," *Electron. Lett.*, vol. 52, no. 20, pp. 1729–1731, Sep. 2016.

[10] A. Younis, R. Mesleh, and H. Haas, "Quadrature spatial modulation performance over Nakagami-*m* fading channels," *IEEE Trans. Veh. Technol.*, vol. 65, no. 12, pp. 10227–10231, Dec. 2016.

[11] O. S. Badarneh and R. Mesleh, "A comprehensive framework for quadrature spatial modulation in generalized fading scenarios," *IEEE Trans. Commun.*, vol. 64, no. 7, pp. 2961–2970, Jul. 2016.

[12] R. Mesleh, S. S. Ikki, and O. S. Badarneh, "Impact of cochannel interference on the performance of quadrature spatial modulation MIMO systems," *IEEE Commun. Lett.*, vol. 20, no. 10, pp. 1927–1930, Oct. 2016.

[13] R. Mesleh, S. Althunibat, and A. Younis, "Differential quadrature spatial modulation," *IEEE Trans. Commun.*, vol. 65, no. 9, pp. 3810–3817, Sep. 2017.

[14] Z. Huang, Z. Gao, and L. Sun, "Anti-eavesdropping scheme based on quadrature spatial modulation," *IEEE Commun. Lett.*, vol. 21, no. 3, pp. 532–535, Mar. 2017.

[15] A. Afana, I. A. Mahady, and S. Ikki, "Quadrature spatial modulation in MIMO cognitive radio systems with imperfect channel estimation and limited feedback," *IEEE Trans. Commun.*, vol. 65, no. 3, pp. 981–990, Mar. 2017.

[16] M. Mohaisen, "Increasing the minimum Euclidean distance of the complex quadrature spatial modulation," *IET Commun.*, vol. 12, no. 7, pp. 854–860, Apr. 2018.

[17] S. Althunibat and R. Mesleh, "Enhancing spatial modulation system performance through signal space diversity," *IEEE Commun. Lett.*, vol. 22, no. 6, pp. 1136–1139, Jun. 2018.
[18] A. Younis, N. Abuzgaia, R. Mesleh, and H. Haas, "Quadrature spatial modulation for 5G outdoor millimeter–wave communications: Capacity analysis," *IEEE Trans. Wireless Commun.*, vol. 16, no. 5, pp. 2882–2890, May 2017.
[19] F. Chen, K. Yang, P. Xing, H. Zhang, and Y. Jiang, "Multiuser pre-coding aided quadrature spatial modulation for large-scale MIMO channels," *China Commun.*, vol. 15, no. 11, pp. 62–69, Nov. 2018.
[20] Y. Wang, T. Zhang, W. Yang, J. Guo, Y. Liu, and X. Shang, "Secure transmission for differential quadrature spatial modulation with artificial noise," *IEEE Access*, vol. 7, pp. 7641–7649, 2019.
[21] Y. Jiang, M. K. Varanasi, and J. Li, "Performance analysis of ZF and MMSE equalizers for MIMO systems: An in-depth study of the high SNR regime," *IEEE Trans. Inf. Theory*, vol. 57, no. 4, pp. 2008–2026, Apr. 2011.
[22] N. I. Miridakis, M. Xia, and T. A. Tsiftsis, "Optimal power allocation and active interference mitigation for spatial multiplexed MIMO cognitive systems," *IEEE Trans. Veh. Technol.*, vol. 67, no. 4, pp. 3349–3360, Apr. 2018.
[23] J. G. Proakis, *Digital Communications*, 4th ed. New York, NY, USA: McGraw-Hill, 2001.
[24] C. Xu, S. Sugiura, S. X. Ng, and L. Hanzo, "Spatial modulation and space-time shift keying: Optimal performance at a reduced detection complexity," *IEEE Trans. Commun.*, vol. 61, no. 1, pp. 206–216, Jan. 2013.
[25] R. Rajashekar, K. V. S. Hari, and L. Hanzo, "Reduced-complexity ML detection and capacity-optimized training for spatial modulation systems," *IEEE Trans. Commun.*, vol. 62, no. 1, pp. 112–125, Jan. 2014.

GUOSHENG HUANG received the M.S. and Ph.D. degrees in computer science from Central South University, China, 2001 and 2010, respectively. He was a Visiting Scholar with Sun Yat-sen University, from 2017 to 2018. He is currently an Associate Professor with the School of Information Science and Engineering, Hunan First Normal University, China. His current research interests include MIMO techniques, wireless sensor networks, and mobile computing.

CHUANPING LI received the M.S. degree in electronics and information technology, Sun Yat-sen University, China, in 2019. His current research interests include MIMO techniques in 5G wireless communications, simultaneous wireless information and power transfer.

SONIA AÏSSA (S'93–M'00–SM'03–F'19) received the Ph.D. degree in electrical and computer engineering from McGill University, Montreal, QC, Canada, in 1998.

Since 1998, she has been with the Institut National de la Recherche Scientifique-Energy, Materials and Telecommunications Center (INRS-EMT), University of Quebec, Montreal, where she is currently a Full Professor. From 1996 to 1997, she was a Researcher with the Department of Electronics and Communications, Kyoto University, and with the Wireless Systems Laboratories, NTT, Japan. From 1998 to 2000, she was a Research Associate with INRS-EMT. From 2000 to 2002, while she was an Assistant Professor, she was a Principal Investigator in the major program of personal and mobile communications of the Canadian Institute for Telecommunications Research, leading research in radio resource management for wireless networks. From 2004 to 2007, she was an Adjunct Professor with Concordia University, Canada. She was a Visiting Invited Professor with Kyoto University, Japan, in 2006, and with Universiti Sains Malaysia, in 2015. Her current research interests include the modeling, design, and performance analysis of wireless communication systems and networks. Dr. Aïssa served as a Distinguished Lecturer of the IEEE Communications Society and a member of its Board of Governors, from 2013 to 2016 and 2014 to 2016, respectively. She received the NSERC University Faculty Award, in 1999; the Quebec Government FRQNT Strategic Faculty Fellowship, in 2001–2006; and the Technical Community Service Award from the FRQNT Centre for Advanced Systems and Technologies in Communications, in 2007. She has been receiving the INRS-EMT Performance Award multiple times, since 2004, for outstanding achievements in research, teaching, and service. She was a co-recipient of five IEEE Best Paper Awards, the 2012 IEICE Best Paper Award, and the NSERC Discovery Accelerator Supplement Award. She was the Founding Chair of the IEEE Women in Engineering Affinity Group, Montreal, from 2004 to 2007; a TPC Symposium Chair or Cochair at IEEE ICC '06 '09 '11 '12; a Program Cochair at IEEE WCNC 2007; a TPC Cochair of IEEE VTCspring 2013; a TPC Symposia Chair of IEEE GLOBECOM 2014; a TPC Vice-Chair of IEEE GLOBECOM 2018; and serves as the TPC Chair of IEEE ICC 2021. She was an Editor of the IEEE TRANSACTIONS ON WIRELESS COMMUNICATIONS, from 2004 to 2012; an Associate Editor and Technical Editor of the *IEEE Communications Magazine*, from 2004 to 2015; a Technical Editor of the IEEE *Wireless Communications Magazine*, from 2006 to 2010; and an Associate Editor of *Security and Communication Networks Journal* (Wiley), from 2007 to 2012. She currently serves as an Area Editor of the IEEE TRANSACTIONS ON WIRELESS COMMUNICATIONS. She is a Fellow of the Canadian Academy of Engineering.

MINGHUA XIA (M'12) received the Ph.D. degree in telecommunications and information systems from Sun Yat-sen University, Guangzhou, China, in 2007.

From 2007 to 2009, he was with the Electronics and Telecommunications Research Institute (ETRI), South Korea, Beijing Research and Development Center, Beijing, China, where he was a member and then as a Senior Member of Engineering Staff. From 2010 to 2014, he was in sequence with The University of Hong Kong, Hong Kong, China; King Abdullah University of Science and Technology, Jeddah, Saudi Arabia; and the Institut National de la Recherche Scientifique (INRS), University of Quebec, Montreal, Canada, as a Postdoctoral Fellow. Since 2015, he has been a Professor with Sun Yat-sen University. His current research interests include wireless communications and signal processing.

Dr. Xia received the Professional Award from the IEEE TENCON, Macau, in 2015. He was recognized as an Exemplary Reviewer by the IEEE TRANSACTIONS ON COMMUNICATIONS, in 2014, the IEEE COMMUNICATIONS LETTERS, in 2014, and the IEEE WIRELESS COMMUNICATIONS LETTERS, in 2014 and 2015. He served as a TPC Symposium Chair of the IEEE ICC'2019 and currently serves as an Associate Editor of the IEEE TRANSACTIONS ON COGNITIVE COMMUNICATIONS AND NETWORKING, and the *IET Smart Cities*.